Benzimidazothiazolone Derivatives

Subjects: Biology

Contributor: Hae Young Chung

Thirteen (Z)-2-(substituted benzylidene)benzimidazothiazolone analogs were synthesized and evaluated for their inhibitory activity against mushroom tyrosinase. Among the compounds synthesized, compounds 1–3 showed greater inhibitory activity than kojic acid (IC50 = 18.27 ± 0.89 μM); IC50 = 3.70 ± 0.51 μM for 1; IC50 = 3.05 ± 0.95 μM for 2; and IC50 = 5.00 ± 0.38 μM for 3, and found to be competitive tyrosinase inhibitors. In silico molecular docking simulations demonstrated that compounds 1–3 could bind to the catalytic sites of tyrosinase. Compounds 1–3 inhibited melanin production and cellular tyrosinase activity in a concentration-dependent manner. Notably, compound 2 dose-dependently scavenged ROS in B16F10 cells. Furthermore, compound 2 downregulated the protein kinase A (PKA)/cAMP response element-binding protein (CREB) and mitogen-activated protein kinase (MAPK) signaling pathways, which led to a reduction in microphthalmia-associated transcription factor (MITF) expression, and decreased tyrosinase, tyrosinase related protein 1 (TRP1), and TRP2 expression, resulting in anti-melanogenesis activity. Hence, compound 2 may serve as an anti-melanogenic agent against hyperpigmentation diseases.

Keywords: tyrosinase inhibitor ; reactive oxygen species (ROS) ; melanogenesis ; benzimidazothiazolone

1. Introduction

Tyrosinase (polyphenol oxidase, EC 1.14.18.1), a binuclear copper-containing monooxygenase, is a critical rate-limiting melanogenic enzyme involved in melanogenesis, the process of melanin synthesis in the skin. Melanogenesis is initiated by the hydroxylation of tyrosine to l-3,4-dihydroxy-phenylalanine (DOPA), which is catalyzed by tyrosinase. Tyrosinase also catalyzes the subsequent enzymatic conversion of DOPA to dopaquinone [1][2]. Tyrosinase is the key factor involved in inducing dermatological disorders, including age spots, freckles, and melasma. Commercial tyrosinase inhibitors, such as hydroquinone, arbutin [3], kojic acid [4], ellagic acid [5], and tranexamic acid, have been used as skin-whitening agents; however, they are associated with certain side effects, including carcinogenicity, chemical instability, and poor bioavailability [6][7]. Thus, novel and efficient, anti-tyrosinase inhibitor with a favorable safety profile are necessary for anti-hyperpigmentation. There is a need to develop safe skin-whitening agents in order to overcome the limitations of established products.

α-Melanocyte-stimulating hormone (α-MSH) and 3-isobutyl-1-methylxanthine (IBMX) are the main physiological inducers of melanogenesis and accelerate tyrosinase activity through the cyclic adenosine monophosphate (cAMP) signaling pathway [8]. Furthermore, α-MSH binds to melanocortin-1 receptors (MC1R) on the surface of melanocytes to activate the protein kinase A (PKA) pathway, phosphorylate the cAMP response element-binding protein (CREB) transcription factor; and induce the expression of microphthalmia-associated transcription factor (MITF), thus promoting melanogenesis [9][10]. Activated MITF induces the expression of melanogenic enzyme genes, such as tyrosinase-related protein 1 (TRP1) and dopachrome tautomerase (TRP2; DCT) [11][12][13]. The PKA/CREB and mitogen-activated protein kinase (MAPK) signaling pathways are important in melanogenesis; therefore, we wondered if chemicals or agents that block or activate this axis could have anti- or pro-melanogenic activity and thus serve as potential therapeutic agents for hyperpigmentation disorders [14][15][16].

Reactive oxygen species (ROS) have been linked to several disorders, including aging and age-related diseases [17][18]. Importantly, ROS levels can accelerate skin aging and increase both melanocyte proliferation and hyperpigmentation [19][20]. Among the reactive species (RS) derived from melanocytes and keratinocytes, nitric oxide (·NO) and superoxide anion radical ($O_2^{\cdot -}$) stimulate melanin synthesis by enhancing the protein expression of tyrosinase and TRP1 [21][22][23][24]. Therefore, antioxidants, inhibitors of tyrosinase, and scavengers of ROS may suppress melanogenesis in the epidermis.

Benzimidazothiazoles, as core rings, are polycyclic isosteres whose derivatives have been reported to exert anticancer [25] and anti-inflammatory [26][27] activities. However, no study has yet described its anti-tyrosinase and hyperpigmenting effects in vitro model. Previously, we reported that (*Z*)-β-phenyl-α,β-unsaturated carbonyl scaffolds inhibit tyrosinase and melanogenesis both in vitro [28][29][30][31]. As our continuous efforts to find potent tyrosinase inhibitors using (*Z*)-β-phenyl-

α,β-unsaturated carbonyl scaffolds, we integrated the benzimidazothiazolone template with other benzaldehydes to synthesize a (*Z*)-β-phenyl-α,β-unsaturated carbonyl scaffold.

2. Results and Discussion on New Benzimidazothiazolone Derivatives

2.1. Synthesis of (Z)-2-(Substituted benzylidene)benzimidazothiazolone Derivatives *1–13*

The synthetic route for the benzimidazothiazolone derivatives **1**–**13** is illustrated in Scheme 1. To synthesize the core template benzimidazothiazolone **15**, commercially available 2-mercaptobenzimidazole was first condensed with bromoacetic acid. The reaction provided the desired compound **15** at a yield of 8%, with an intermediate **14** (59%). In the presence of acetic anhydride and pyridine, the intermediate **14** could be converted to the core template **15** rapidly and in high yield (91%) under reflux. Heating **15** and various benzaldehydes in the presence of acetic acid and sodium acetate for 15 h to 3 days produced 13 benzimidazothiazolone derivatives **1**–**13** as solids in yields of 35–82%. The configuration of the newly formed double bond was determined using the vicinal ^{1}H and ^{13}C-coupling constants (^{3}J) in the proton-coupled ^{13}C spectra.

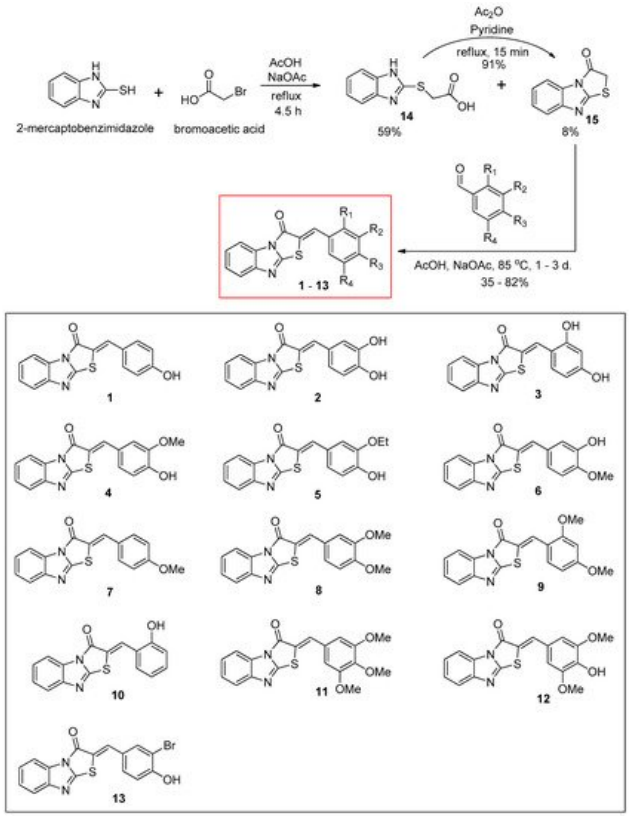

Scheme 1. Synthesis scheme of (*Z*)-2-(substituted benzylidene)benzimidazothiazolone derivatives **1**–**13**.

Vögeli et al. [32] reported that the configuration of trisubstituted exocyclic C, C-double bonds in a general structure A (**Figure 1**) differentiated the C, H-spin coupling constants over three bonds. The ^{3}J of C(1) of compounds in which the oxygen of carbonyl and the 3-hydrogen were on the same side was 3.6 to 6.4 Hz, whereas that of the compounds in which the oxygen of carbonyl and 3-hydrogen were on the same side was roughly twice as large (generally >10 Hz). The ^{3}J of C(1) of compound **11** was 5.3 Hz, confirming that **11** is a (*Z*)-isomer. Structures of the 13 final compounds were confirmed with ^{1}H and ^{13}C NMR spectroscopy and mass spectroscopy.

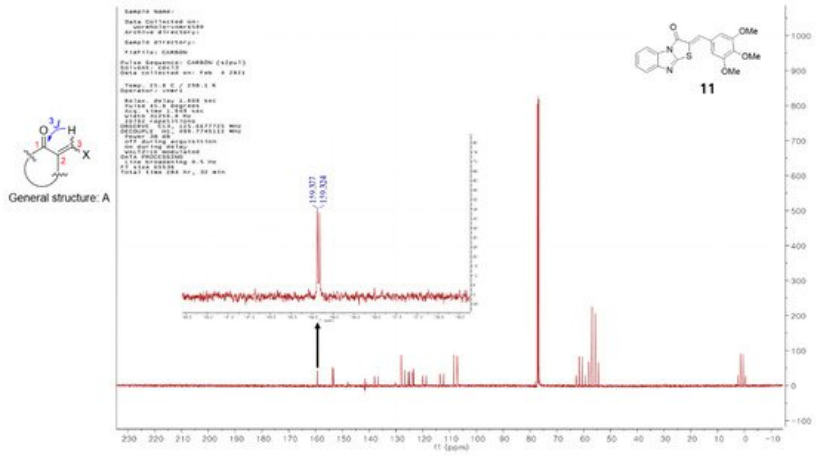

Figure 1. General structure of derivatives with trisubstituted exocyclic C, C-double bond, and the proton-coupled ^{13}C spectrum of compound **11**.

2.2. Inhibitory Activities of (Z)-2-(Substituted Benzylidene)benzimidazothiazolone Derivatives *1–13* against Mushroom Tyrosinase

To choose potent derivatives for cell-based in vitro of anti-tyrosinase and melanogenic-inhibitory activity, we synthesized 13 (*Z*)-2-(substituted benzylidene)benzimidazothiazolone derivatives **1**–**13**, which were determined using mushroom tyrosinase and kojic acid (as a potent tyrosinase inhibitor) [33][34]. The inhibitory potential of compounds **1**–**13** against tyrosinase was assessed using l-tyrosine as the substrate, and the results were described as the IC_{50} values determined with linear regression analysis (**Table 1**). Of the 13 synthesized compounds, three exhibited potent tyrosinase inhibitor; **1** (IC_{50} = 3.70 μM) with a 4-hydroxy substituent; **2** (IC_{50} = 3.05 μM) with a 3,4-dihydroxy substituent; and **3** (IC_{50} = 5.00 μM) with a 2,4-dihydroxy substituent. Specifically, the inhibitory potencies of compounds **1**, **2**, and **3** were 4.9-, 6.0-, and 3.7-fold greater, respectively, than those of kojic acid (IC_{50} = 18.27 μM). Compounds **4**, **5**, **8**, **10**, **11**, and **13** showed moderate inhibitory activities, with IC_{50} values of 42.06 μM, 21.03 μM, 41.40 μM, 27.96 μM, 34.10 μM, and 34.60 μM, respectively. Compounds **6**, **7**, **9**, and **12** were inactive at the tested concentrations.

Table 1. Mushroom tyrosinase inhibitory activity of (*Z*)-2-(substituted benzylidene) benzimidazothiazolone derivatives **1**–**13**.

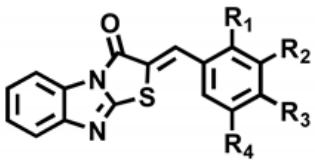

Compounds 1 - 13

Compounds	R_1	R_2	R_3	R_4	IC_{50} Values [a] (μM)
1	**H**	**H**	**OH**	**H**	**3.70 ± 0.51**
2	**H**	**OH**	**OH**	**H**	**3.05 ± 0.95**
3	**OH**	**H**	**OH**	**H**	**5.00 ± 0.38**
4	**H**	**OMe**	**OH**	**H**	**42.06 ± 4.28**
5	**H**	**OEt**	**OH**	**H**	**21.03 ± 0.82**
6	**H**	**OH**	**OMe**	**H**	**NI [b]**
7	**H**	**H**	**OMe**	**H**	**NI**
8	**H**	**OMe**	**OMe**	**H**	**41.40 ± 0.68**
9	**OMe**	**H**	**OMe**	**H**	**NI**
10	**OH**	**H**	**H**	**H**	**27.96 ± 1.32**
11	**H**	**OMe**	**OMe**	**OMe**	**34.10 ± 4.06**
12	**H**	**OMe**	**OH**	**OMe**	**53.55 ± 4.71**

Compounds	R_1	R_2	R_3	R_4	IC_{50} Values [a] (μM)
13	**H**	**Br**	**OH**	**H**	**34.60 ± 2.32**
Kojic acid [c]					**18.27 ± 0.89**

[a] Half-maximal inhibitory concentration (IC_{50}) is expressed as the mean ± standard error of the mean (SEM) of triplicate experiments. [b] NI: no inhibition. [c] Positive control.

Insertion of an additional hydroxyl group into the β-phenyl ring of compound **1** with a 4-hydroxyphenyl ring increased tyrosinase inhibitory activity (compounds **1** vs. **2** and **3**). Furthermore, the introduction of methoxyl, ethoxyl, or bromo groups at the 3-position of the β-phenyl ring of compound **1** with a 4-hydroxyphenyl ring abated tyrosinase inhibitory activity (compounds **1** vs. **4** and **5** and **13**). Compounds **7**, **8**, **9**, and **11,** without a hydroxyl group on the β-phenyl ring showed weak or no inhibition. The 3-methoxy-4-hydroxy group of the β-phenyl ring increased tyrosinase inhibitory activity compared to the 3-hydroxy-4-methoxy group of the β-phenyl ring (compounds **4** vs. **6**). Unlike the hydroxyl group, 2,4-dimethoxyphenyl groups act as hydrogen bond acceptors and are very weak or inactive. The present results are in close agreement with those of a previous reported [35].

Based on the results of our previous studies, 3,4-dihydroxyphenyl compound exhibit potent inhibitory activity against mushroom tyrosinase and cell-based cellular tyrosinase assays [36]. As expected, compound **2**, with a 3,4-dihydroxyphenyl substituent (catechol moiety), exerted excellent tyrosinase inhibition, and compounds with 4-hydroxyphenyl (**1**) and 2,4-dihydroxyphenyl (**3**, resorcinol moiety) substituents also exerted potent tyrosinase inhibition. These results indicate that the 4-substitueted resorcinol moiety importantly confers tyrosinase inhibiting activity.

The position and number of hydroxyl substituents on the phenyl ring significantly influenced the inhibitory activity against tyrosinase. However, the details of certain chemical structures attached to the one or two hydroxyphenyl moieties for tyrosinase activity remain unknown; this will be the focus of future research.

2.3. Enzyme Kinetic Studies of Compounds *1*–*3*

To elucidate the type of enzymatic inhibition, a kinetic analysis was accomplished at several concentrations of the l-tyrosine substrate and inhibitors (**1**–**3**), according to the Lineweaver–Burk and Dixon plot methods (**Table 2** and **Figure 2**). Kojic acid, a competitive tyrosinase inhibitor, was used as the standard [34]. Using the Lineweaver–Burk plot method, the lines representing inhibitors **1**–**3** intersected at the same point on the *y*-axis, demonstrating that *Km* increased with increasing concentrations of inhibitors **1**–**3**, while $1/V_{max}$ did not change [37]. Compounds **1**–**3** showed competitive inhibition. These data suggest that compounds **1**–**3** are effective inhibitors that bind to the active site of the enzyme [7]. Furthermore, the Dixon plot is a graphical method [plot of 1/enzyme velocity (1/*V*) against inhibitor concentration (I)] used to determine the type of enzymatic inhibition and the dissociation or inhibition constant (K_{ic}) for the enzyme-inhibitor complex [37].

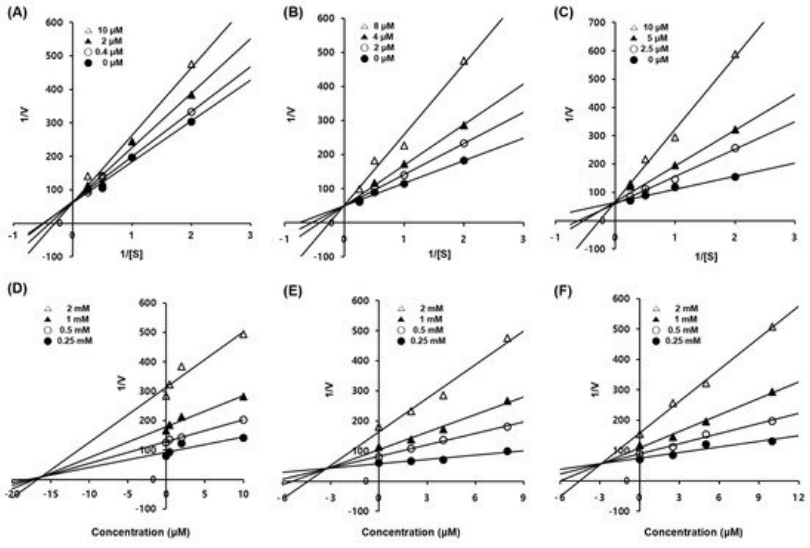

Figure 2. Enzymatic kinetics study of compounds **1**–**3** against tyrosinase. Lineweaver–Burk plots for the inhibition of mushroom tyrosinase of compounds **1** (**A**), **2** (**B**), and **3** (**C**). Dixon plots for tyrosinase inhibition of compounds **1** (**D**), **2** (**E**), and **3** (**F**) using l-tyrosine as the substrate. Data are presented as the mean values of 1/*V*, defined as the inverse of increased absorbance at 492 nm, as determined at several different l-tyrosine concentrations (0.5, 1, 2 and 4 mM).

Table 2. Kinetic studies of compounds **1**–**3** against mushroom tyrosinase.

Compounds	Inhibition Type [a]	K_{ic} Values (μM) [b]
1	**Competitive**	**16.55**
2	**Competitive**	**3.21**
3	**Competitive**	**3.01**
Kojic acid [c]	**–**	**–**

[a] Determined using Lineweaver–Burk plots. [b] Determined using Dixon plots. [c] Positive control. (–) No test.

The K_{ic} (≈K_i) values for compounds **1**–**3** were 16.55, 3.21, and 3.01 μM, respectively, against mushroom tyrosinase (**Table 3** and **Figure 2**). As the K_{ic} value represents the concentration required to combine the inhibitor with an enzyme, compounds with lower K_{ic} values were generally more effective tyrosinase inhibitors; this is an important requisite for the development of preventive and therapeutic agents.

2.4. Docking Simulation and of Ligands against Tyrosinase

Based on the in vitro results, compound **1**–**3**—docking complexes were evaluated to understand their binding conformation within the active site of the tyrosinase. To predict the binding site of the potent compounds **1**–**3**, molecular docking simulations were performed using the open-source programs for AutoDock4.2 [38] and AutoDock Vina [39] along with AutoDockTools, a graphical user interface compliment to the AutoDock software suite. AutoDock 4.0 uses a semi-empirical free energy force field to predict the binding free energies of protein–ligand complexes of a known structure and the binding energy for both bound and unbound states [38]. AutoDock vina was developed as a successor to AutoDock 4.2 and provides more rapid and accurate results with less direct investment required by the end user [40].

The most important factor involved in tyrosinase inhibition are coordinated with Cu ions, which played an important role in the activity. The binding energy, number of interaction residues of the compounds, and the reference compound kojic acid (competitive inhibitor) (**Figure 3**B) [41][42] are summarized in **Table 3** and **Figure 3**A. The most potent compound **2** was stabilized by HIS85-, HIS244-, ASN260-, HIS263-, PHE264-, MET280-, GLY281-, SER282-, VAL283-, and GLU322-interacting (hydrogen/hydrophobic) residues (**Figure 3**D,G). Similarly, compound **1-** or compound **3**-tyrosinase complexes interacted with HIS61, HIS85, HIS259, HIS263, PHE264, ARG268, GLY281, SER282, VAL283, ALA286, and PHE292 residues, as shown in **Figure 3**C,F for compound **1**; and **Figure 3**E,H for compound **3**. The residues of active site of tyrosinase are HIS61, HIS85, HIS94, His259, HIS263, VAL283, and HIS296, detailed results for searching active site of tyrosinase have been previously reported [43], which also partially observed in our compounds **1**–**3**. The binding energies of –6.73/–6.3, –6.92/–6.5, –6.35/–6.4 kcal/mol were consumed by compounds **1**–**3**, as determined using the AutoDock 4.2 and AutoDock Vina programs. The binding scores of kojic acid were –4.21/–5.6 kcal/mol, indicating that compounds **1**–**3** may be bind to tyrosinase with stronger affinity than kojic acid. The basic skeleton of the synthesized compounds was similar; therefore, no significant difference in energy value was observed between the docking results. Data from the literature have also confirmed the importance of HIS259 and HIS263 residues in bonding with other tyrosinase inhibitors, supporting our docking results [43][44][45].

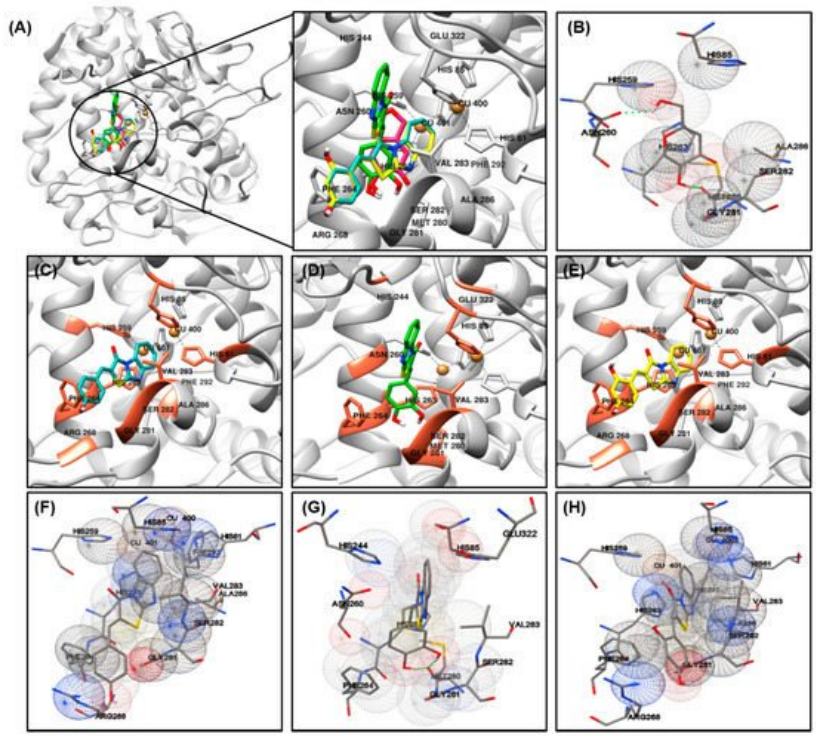

Figure 3. Molecular docking simulations of tyrosinase inhibition by the reference compound and compounds **1** ((**C**), blue stick), **2** ((**D**), green stick), and **3** ((**E**), yellow stick) in the active site of *Agaricus bisporus* mushroom tyrosinase (PBD ID: 2Y9X) (**A**). The binding residues of kojic acid (**B**) and compounds **1** (**F**), **2** (**G**), and **3** (**H**) with tyrosinase were analyzed using the AutoDockTools software. Oxygen and nitrogen atoms are displayed in red and blue, respectively. Copper ions are shown in orange.

Table 3. Docking energy and binding sites of compounds **1**–**3** against mushroom tyrosinase (PDB ID: 2Y9X), as performed using the AutoDock 4.2 and AutoDock Vina programs.

Compounds	Binding Energy (kcal/mol) [a]		Interaction with Amino Acid Residues [b]
	AutoDock 4.2	AutoDock Vina	
1	**−6.73**	**−6.3**	**HIS61, HIS85, HIS259, HIS263, PHE264, ARG268, GLY281, SER282, VAL283, ALA286, PHE292.**
2	**−6.92**	**−6.5**	**HIS85, HIS244, ASN260, HIS263, PHE264, MET280, GLY281, SER282, VAL283, GLU322.**
3	**−6.35**	**−6.4**	**HIS61, HIS85, HIS259, HIS263, PHE264, ARG268, GLY281, SER282, VAL283, ALA286, PHE292.**
Kojic acid [c]	**−4.21**	**−5.6**	**HIS85, HIS259, ASN260, HIS263, MET280, GLY281, SER282, ALA286.**

[a] Binding energy indicates the binding affinity and capacity for the active site of mushroom tyrosinase enzyme. [b] All amino acid residues of the enzyme-inhibitor complex were determined using the AutoDock 4.2 and AutoDock vina programs. [c] Reported competitive-type inhibitors.

2.5. Cell Viability of Compounds *1*–*3*

The anti-melanogenic activity of compounds **1**–**3**, which were the most effective in B16F10 cells, was tested in a cell-based in vitro model. The EZ-Cytox assay was used to estimate cell viability. Cells were treated with various concentrations (5–200 μM) of compounds **1**–**3** and trolox to examine whether these compounds exhibited cytotoxic effects on melanocytes. The results indicated that compounds **1**–**3** and trolox did not significantly affect cell viability at concentrations up to 20 μM compared with the vehicle control cells for 48 h (**Figure 4**). Consequently, 20 μM sample concentrations of compounds **1**–**3** and trolox were used for further experiments.

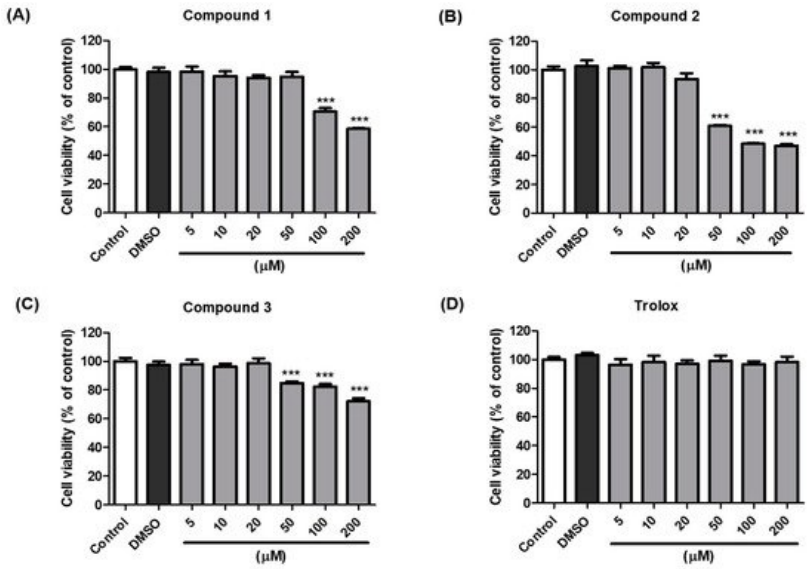

Figure 4. Effects of compounds **1**–**3** and trolox on the viability of B16F10 cells. Cells were incubated with different concentrations (5–200 μM) of compound **1** (**A**), **2** (**B**), **3** (**C**), and trolox (**D**) for 48 h, and cell viability was determined using EZ-Cytox assay. *** $p < 0.001$ vs. DMSO-treated.

2.6. ROS Scavenging Activity

ROS may regulate melanogenesis in melanoma cells [20][46][47]. The principle of the intracellular ROS assay is that DCF-DA spreads through the cell membrane and is enzymatically hydrolyzed to DCF by esterase; DCFH then responses with ROS to yield DCF [48]. The ROS scavenging activity of compounds **1**–**3** was investigated in vitro by using fluorescence probes, (DCF-DA) for ROS. SIN-1 is used as an NO donor [49][50]. As demonstrated in **Figure 5**A, compound **2** exerted potent scavenging activity against ROS, with an IC_{50} value of 2.36 ± 0.48 μM, comparable with that of the reference control, trolox, which had an IC_{50} value of 13.25 ± 0.73 μM. However, compounds **1** and **3** did not present any activity at the tested concentrations at ≥50 μM. Furthermore, as shown in **Figure 5**B, treatment with SIN-1 significantly increased ROS generation compared to that in untreated B16F10 cells. Pretreatment with compound **2** reduced SIN-1-induced ROS generation in a dose-dependent manner. These results indicated that compound **2** attenuated the SIN-1-induced increase in ROS activity and intracellular ROS levels. Structure comparison of the benzimidaxothiazolone skeleton and ROS scavenging activities reveals that a *ortho*-dihydroxy groups of the benzylidene plays a crucial role in the observed scavenging activity. The importance of catechol moiety (3,4-dihydroxy group) for ROS scavenging activity was reported in previous studies in the literature [51][52].

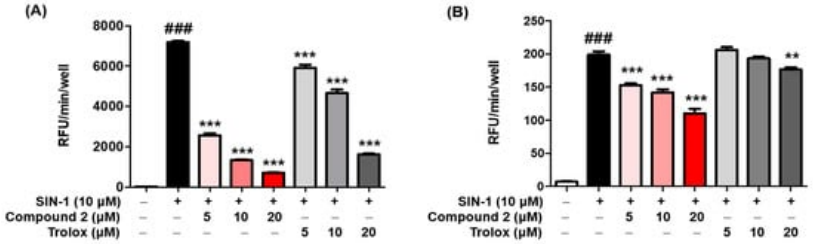

Figure 5. Reactive oxygen species (ROS) scavenging activity of compound **2**. The inhibitory effect of compound **2** on ROS production was evaluated. A DCFDA assay was performed to determine ROS levels. The ROS scavenger trolox was used as the positive control. The scavenging activity of compound **2** on oxidative stress induced by 10 μM SIN-1 was estimated in cell-free in vitro (**A**). B16F10 cells were pre-treated with compound **2** and trolox for 3 h and further treated with 10 μM SIN-1 (**B**). Data are presented as the mean ± SEM. ### $p < 0.001$ vs. control. ** $p < 0.01$ and *** $p < 0.001$ vs. SIN-1-treated or SIN-1-treated cells, respectively.

2.7. Melanin Contents and Cellular Tyrosinase Assay

α-MSH and IBMX increase the levels of intracellular cAMP, which induces melanogenesis [9][53][54]. Melanin contents were measured after pretreating the B16F10 cells with different concentrations (5, 10, and 20 μM) of the compounds **1**–**3** for 3 h, followed by 48 h of α-MSH and IBMX treatment. The melanin contents increased to 134.78 ± 2.95%, 137.96 ± 3.02%, and 134.78 ± 2.95% (**Figure 6**A–C, respectively) following treatment with α-MSH and IBMX. As shown in **Figure 6**B, compound **2** led to a dose-dependent decrease in the intracellular tyrosinase activity to 116.75 ± 3.52%, 100.52 ± 2.08%, and 78.80 ± 3.66%. Kojic acid at 20 μM reduced the content to 128.53 ± 2.95%. In parallel to the enzyme assay, compound **1** reduced the melanin content at 20 μM (**Figure 6**A), and compound **3** increased the melanin contents in a

dose-dependent manner (**Figure 6**C). To determine the inhibitory potency of compounds **1**–**3** in the cellular model system, the inhibitory effect on the tyrosinase activity of B16F10 cells treated with 5 μM α-MSH and 200 μM IBMX were examined. The level of intracellular tyrosinase after α-MSH and IBMX treatment was 347.03 ± 7.97%, 356.28 ± 27.70%, and 341.30 ± 26.76% (**Figure 6**D–F, respectively). However, cellular tyrosinase activity decreased in a concentration-dependent manner upon exposure to compounds **1**–**3**. In both melanin contents and cellular tyrosinase inhibitory assay, compound **2** exhibited potent inhibitory activities, indicating that the presence of 3,4-dihydroxy (catechol moiety) substituent of benzimidaxothiazolone derivatives influence inhibitory activity. These results suggest that compound **2** is a promising candidate therapeutic anti-melanogenesis agent among benzimidazothiazolone derivatives.

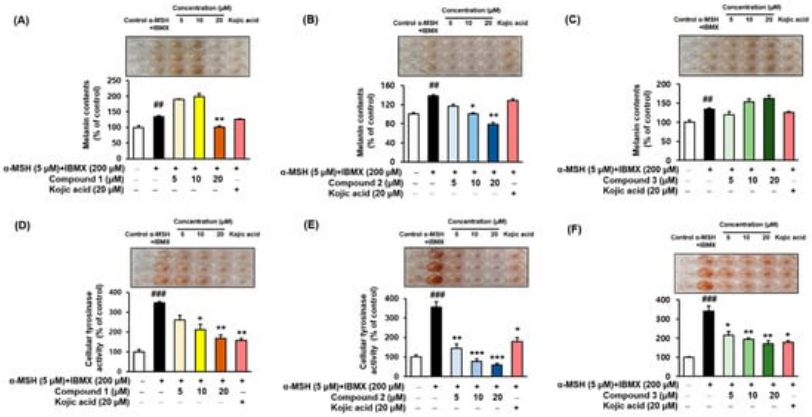

Figure 6. Effects of compounds **1**–**3** on the cellular melanin contents (**A**–**C**) and tyrosinase inhibitory activities (**D**–**F**) of α-MSH and IBMX-induced B16F10 cells, respectively. Cells were pre-incubated for 24 h and then stimulated with α-MSH (5 μM) and IBMX (200 μM) in the presence of compounds **1**–**3** (5, 10, and 20 μM) or kojic acid (20 μM) for 48 h. Data are presented as the mean ± SEM of three independent experiments. ## $p < 0.01$ and ### $p < 0.001$ vs. control. * $p < 0.05$, ** $p < 0.01$, and *** $p < 0.001$ vs. α-MSH and IBMX-treated cells.

2.8. Effects of Compound *2* on Melanogenesis-Related Signaling

It is important to determine whether the inhibition of melanin synthesis by compound **2** is related to melanogenesis signaling and gene expression. To investigate whether compound **2** could affect the melanogenic signaling of tyrosinase, the expression of tyrosinase, phosphorylated CREB and PKA was determined with Western blot analysis using cytosolic factions from the cell lysates of α-MSH- and IBMX-induced B16F10 cells. As shown in **Figure 7**A,B, treatment with α-MSH and IBMX significantly upregulated these proteins; however, compound **2** decreased their expression on these proteins in a dose-dependent manner. MITF, a leucine zipper transcription factor, activates the expression of multiple genes encoding enzymes involved in the conversion of tyrosine into melanin, resulting in increased levels of these melanin-producing proteins [55][56]. Expression of MITF in α-MSH- and IBMX-induced B16F10 cells was upregulated, while compound **2** significantly suppressed MITF levels in the nuclear faction from total cell lysate (**Figure 7**C). The skin is site of oxidative stress due to exposure to daylight and environmental oxidizing pollutants. It is known that ROS stimulates α-MSH- and IBMX-induced production in melanoma cells leading to melanogenesis by upregulating MITF, a transcription factor that induces tyrosinase gene expression [57][58]. Since oxidative stress has been shown to activate MITF through MAPK, we investigated whether compound **2** controls MAPK signaling [59][60]. The results shown in **Figure 7**D,E revealed that compound **2** decreased the levels of phosphorylated JNK and ERK in a concentration-dependent manner. However, the levels of phosphorylated p38 were not affected by treatment with compound **2**. In our study, both p-JNK and p-ERK were decreased by compound **2**. Thus, our results suggest that compound **2**, which suppresses the phosphorylated PKA and MAPK signaling pathways and MITF-mediated melanogenic enzyme expression, has potential as an anti-melanogenic agent.

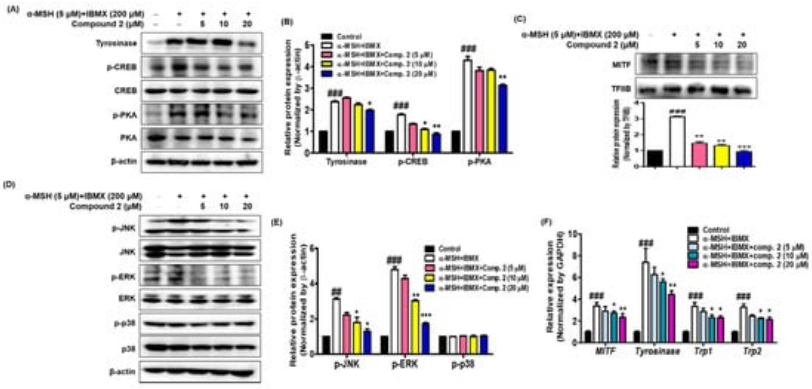

Figure 7. Effects of compound **2** on melanogenic proteins and mRNA levels in α-MSH- and IBMX-induced B16F10 cells. Cells were pre-incubated for 24 h and then stimulated with α-MSH (5 μM) and IBMX (200 μM) in the presence of compound **2** (5, 10, and 20 μM). The expression levels of tyrosinase, p-CREB, p-PKA, p-JNK, p-ERK, p-p38, and β-actin were determined with Western blotting in the cytosolic fraction. β-actin was used as the loading control (**A**,**B**,**D**,**E**). The expression levels of MITF and TFIIB were determined with Western blotting in the nuclear fraction. TFIIB was used as the loading control (**C**). Relative mRNA levels of the melanogenic genes *MITF*, *Tyrosinase*, *Trp1*, and *Trp2* in the cells were quantified using real-time qPCR and normalized to the *GAPDH* mRNA level (**F**). The primer sets are shown in **Table 1**. Data are presented as the mean ± SEM of three independent experiments. ## $p < 0.01$ and ### $p < 0.001$ vs. control. * $p < 0.05$, ** $p < 0.01$, and *** $p < 0.001$ vs. α-MSH and IBMX-treated cells.

The effects of compound **2** on the expression of mRNA melanogenic factors were evaluated in α-MSH- and IBMX-induced B16F10 cells. Total mRNAs were extracted from cells treated with α-MSH and IBMX in the absence or presence of compound **2**. Tyrosinase, TRP1 and TRP2 are key enzymes involved in melanin biosynthesis [56]. During melanin synthesis, tyrosine undergoes tyrosinase-dependent conversion, which is catalyzed by dapaquinone and subsequently by dopachrome. TRP2 converts dopachrome to 5,6-dihydroxyindole-2-carboxylic acid (DHICA), whereas TRP1 oxidizes DHICA to a carboxylated indole-quinone, which is eventually converted into melanin [12][60][61]. The mRNA levels of tyrosinase, TRP1, TRP2, and MITF were quantified with real-time qPCR (**Figure 7**F). Compound **2** significantly inhibited the expression of the MITF and downstream enzymes, such as tyrosinase, TRP1, and TRP2. These results indicate that compound **2** might be an effective hypopigmenting agent with implications in various dermatologic hyperpigmentation disorders, such as freckles and melasma, and has useful effects in whitening cosmetic agents.

3. Conclusions

To determine whether benzimidazothiazolone with a (*Z*)-β-phenyl-α,β-unsaturated carbonyl scaffold plays an important role in tyrosinase inhibition, 13 derivatives were synthesized. The mushroom tyrosinase inhibitory assay revealed that three benzimidazothiazolone derivatives (compounds **1**–**3**) with 4-, 3,4-, and 2,4-dihydroxyls on the phenyl ring of the benzimidazothiazolone scaffold, respectively, inhibited tyrosinase significantly more than the positive control (kojic acid). Enzymatic kinetic studies indicated that compounds **1**–**3** were competitive inhibitors. Docking simulation of compounds **1**–**3** predicted that they bind more strongly to the active site of tyrosinase than kojic acid. In vitro experiments showed that compounds **1**–**3** inhibited cellular tyrosinase inhibitory activity in a dose-dependent manner. Compound **2** scavenged ROS and inhibited melanin biosynthesis downregulating the PKA/CREB and MAPK signaling pathways, leading to suppression of MITF expression and tyrosinase (**Figure 8**). This is the first report of benzimidazothiazolone with a (*Z*)-β-phenyl-α,β-unsaturated carbonyl scaffold for anti-tyrosinase and anti-melanogenesis effects to the best our knowledge.

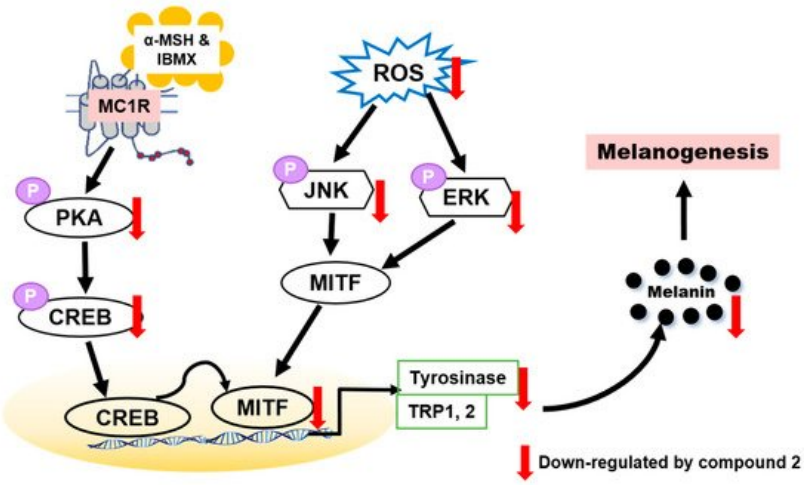

Figure 8. Proposed mechanism of action of compound **2** against melanogenesis.

In the present study, it was found that compound **2** suppressed intracellular ROS level in a dose-dependent manner. Compound **2** appears to be a potential whitening agent that might protect melanoma cells from oxidative injury. Hence, compound **2** has potential for use as a novel dermatological anti-melanogenesis agent and an effective skin-whitening agent. Although many synthetic inhibitors exhibited remarkable tyrosinase inhibitory activity, only a few of them showed melanogenesis inhibition activity in cell-based or skin models. Therefore, further studies may be required to assess the potential for developing safe products of skin-whitening agents by in vivo studies [62], such as zebra fish, and may have practical applications for humans.

References

1. Decker, H.; Tuczek, F. Tyrosinase/catecholoxidase activity of hemocyanins: Structural basis and molecular mechanism. Trends Biochem. Sci. 2000, 25, 392–397.
2. Kang, S.J.; Choi, B.R.; Lee, E.K.; Kim, S.H.; Yi, H.Y.; Park, H.R.; Song, C.H.; Lee, Y.J.; Ku, S.K. Inhibitory effect of dried pomegranate concentration powder on melanogenesis in B16F10 melanoma cells; involvement of p38 and PKA signaling pathways. Int. J. Mol. Sci. 2015, 16, 24219–24242.
3. Nakajima, M.; Shinoda, I.; Fukuwatary, Y.; Hayahawa, H. Arbutin increases the pigmentation of cultured human melanocytes through mechanisms other than the induction of tyrosinase activity. Pigment Cell Res. 1998, 11, 12–17.
4. Takizawa, T.; Imai, T.; Onose, J.-I.; Ueda, M.; Tamura, T.; Mitsumori, K.; Izumi, K.; Hirose, M. Enhancement of hepatocarcinogenesis by kojic acid in rat two-stage models after initiation with N-bis(2-hydroxypropyl)nitrosamine or N-diethylnitrosamine. Toxicol. Sci. 2004, 81, 43–49.
5. Arulmozhi, V.; Pandian, K.; Mirunalini, S. Ellagic acid encapsulated chitosan nanoparticles for drug delivery system in human oral cancer cell line (KB). Colloids Surf. B Biointerfaces 2013, 110, 313–320.
6. Chang, T.S. An updated review of tyrosinase inhibitors. Int. J. Mol. Sci. 2009, 10, 2440–2475.
7. Pillaiyar, T.; Manickam, M.; Namasivayam, V. Skin whitening agents: Medicinal chemistry perspective of tyrosinase inhibitors. J. Enzym. Inhib. Med. Chem. 2017, 32, 403–425.
8. Han, H.J.; Park, S.K.; Kang, J.Y.; Kim, J.M.; Yoo, S.K.; Heo, H.J. Anti-melanogenic effect of ethanolic extract of Sorghum bicolor on IBMX-induced melanogenesis in B16/F10 melanoma cells. Nutrients 2020, 12, 832.
9. Rzepka, Z.; Buszman, E.; Beberok, A.; Wrześniok, D. From tyrosine to melanin: Signaling pathways and factors regulating melanogenesis. Postepy Hig. Med. Dosw. 2016, 70, 695–708.
10. Park, S.Y.; Jin, M.L.; Kim, Y.H.; Kim, Y.; Lee, S.J. Aromatic-turmerone inhibits α-MSH and IBMX-induced melanogenesis by inactivating CREB and MITF signaling pathways. Arch. Dermatol. Res. 2011, 303, 737–744.
11. Jiménez-Cervantes, C.; Solano, F.; Kobayashi, T.; Urabe, K.; Hearing, V.J.; Lozano, J.A.; García-Borrón, J.C. A new enzymatic function in the melanogenic pathway. The 5,6-dihydroxyindole-2-carboxylic acid oxidase activity of tyrosinase-related protein-1 (TRP1). J. Biol. Chem. 1994, 269, 17993–18000.
12. Tachibana, M. MITF: A stream flowing for pigment cells. Pigment Cell Res. 2000, 13, 230–240.
13. D'Mello, S.A.; Finlay, G.J.; Baguley, B.C.; Askarian-Amiri, M.E. Signaling pathways in melanogenesis. Int. J. Mol. Sci. 2016, 7, 1144.
14. Kang, H.Y.; Suzuki, I.; Lee, D.J.; Ha, J.; Reiniche, P.; Aubert, J.; Deret, S.; Zugaj, D.; Voegel, J.J.; Ortonne, J.P. Transcriptional profiling shows altered expression of wnt pathway- and lipid metabolism-related genes as well as melanogenesis-related genes in melasma. J. Investig. Dermatol. 2011, 131, 1692–1700.
15. Bang, S.; Won, K.H.; Moon, H.R.; Yoo, H.; Hong, A.; Song, Y.; Chang, S.E. Novel regulation of melanogenesis by adiponectin via the AMPK/CRTC pathway. Pigment Cell Melanoma Res. 2017, 30, 553–557.
16. Yun, C.Y.; Ko, S.M.; Choi, Y.P.; Kim, B.J.; Lee, J.; Kim, J.M.; Kim, J.Y.; Song, J.Y.; Kim, S.H.; Hwang, B.Y.; et al. α-Viniferin improves facial hyperpigmentation via accelerating feedback termination of cAMP/PKA-signaled phosphorylation circuit in facultative melanogenesis. Theranostics 2018, 8, 2031–2043.
17. Finkel, T.; Holbrook, N.J. Oxidants, oxidative stress and the biology of ageing. Nature 2000, 408, 239–247.
18. Jung, H.J.; Kim, S.M.; Kim, D.H.; Bang, E.; Kang, D.; Lee, S.; Chun, P.; Moon, H.R.; Chung, H.Y. 2,4-Dihydroxyphenyl-benzothiazole (MHY553), a synthetic PPARα agonist, decreases age-associated inflammatory responses through PPARα activation and RS scavenging in the skin. Exp. Gerontol. 2021, 143, 111153.
19. Masaki, H. Role of antioxidants in the skin: Anti-aging effects. J. Dermatol. Sci. 2010, 58, 85–90.
20. Liu, G.S.; Peshavariya, H.; Higuchi, M.; Brewer, A.C.; Chang, C.W.T.; Chan, E.C.; Dusting, G.J. Microphthalmia-associated transcription factor modulates expression of NADPH oxidase type 4: A negative regulator of melanogenesis. Free Radic. Biol. Med. 2012, 52, 1835–1843.
21. Roméro-Graillet, C.; Aberdam, E.; Clément, M.; Ortonne, J.P.; Ballotti, R. Nitric oxide produced by ultraviolet-irradiated keratinocytes stimulates melanogenesis. J. Clin. Invest. 1997, 99, 635–642.
22. Sasaki, M.; Horikoshi, T.; Uchiwa, H.; Miyachi, Y. Up-regulation of tyrosinase gene by nitric oxide in human melanocytes. Pigment Cell Res. 2000, 13, 248–252.
23. Zhou, S.; Sakamoto, K. Pyruvic acid/ethyl pyruvate inhibits melanogenesis in B16F10 melanoma cells through PI3K/AKT, GSK3β, and ROS-ERK signaling pathways. Genes Cells 2019, 24, 60–69.

24. Miao, F.; Su, M.Y.; Jiang, S.; Luo, L.F.; Shi, Y.; Lei, T.C. Intramelanocytic acidification plays a role in the antimelanogenic and antioxidative properties of vitamin C and its derivatives. Oxid. Med. Cell. Longev. 2019, 2019, 2084805.

25. Noha, R.M.; Abdelhameid, M.K.; Ismail, M.M.; Mohammed, M.R.; Salwa, E. Design, synthesis and screening of benzimidazole containing compounds with methoxylated aryl radicals as cytotoxic molecules on (HCT-116) colon cancer cells. Eur. J. Med. Chem. 2021, 209, 112870.

26. Fenichel, R.L.; Alburn, H.E.; Schreck, P.A.; Bloom, R.; Gregory, F.J. Immunomodulating and antimetastatic activity of 3-(p-chlorophenyl) thiazolobenzimidazole-2-acetic acid (Wy-18, 251, Nsc 310633). J. Immunopharmacol. 1980, 2, 491–508.

27. El-Kerdawy, M.M.; Ghaly, M.A.; Darwish, S.A.; Abdel-Aziz, H.A.; Elsheakh, A.R.; Abdelrahman, R.S.; Hassan, G.S. New benzimidazothiazole derivatives as anti-inflammatory, antitumor active agents: Synthesis, in-vitro and in-vivo screening and molecular modeling studies. Bioorg. Chem. 2019, 83, 250–261.

28. Kim, H.R.; Lee, H.J.; Choi, Y.J.; Park, Y.J.; Woo, Y.; Kim, S.J.; Park, M.H.; Lee, H.W.; Chun, P.; Chung, H.Y.; et al. Benzylidene-linked thiohydantoin derivatives as inhibitors of tyrosinase and melanogenesis: Importance of the β-phenyl-α,β-unsaturated carbonyl functionality. MedChemComm 2014, 5, 1410–1417.

29. Ullah, S.; Son, S.; Yun, H.Y.; Kim, D.H.; Chun, P.; Moon, H.R. Tyrosinase inhibitors: A patent review (2011–2015). Expert Opin. Ther. Pat. 2016, 26, 347–362.

30. Jung, H.J.; Lee, M.J.; Park, Y.J.; Noh, S.G.; Lee, A.K.; Moon, K.M.; Lee, E.K.; Bang, E.J.; Park, Y.J.; Kim, S.J.; et al. A novel synthetic compound, (Z)-5-(3-hydroxy-4-methoxybenzylidene)-2-iminothiazolidin-4-one (MHY773) inhibits mushroom tyrosinase. Biosci. Biotechnol. Biochem. 2018, 1–9.

31. Kim, S.J.; Yang, J.; Lee, S.; Park, C.; Kang, D.; Akter, J.; Ullah, S.; Kim, Y.J.; Chun, P.; Moon, H.R. The tyrosinase inhibitory effects of isoxazolone derivatives with a (Z)-β-phenyl-α, β-unsaturated carbonyl scaffold. Bioorg. Med. Chem. 2018, 26, 3882–3889.

32. Vögeli, U.; von Philipsborn, W.; Nagarajan, K.; Nair, M.D. Structures of addition products of acetylenedicarboxylic acid esters with various dinucleophiles. An application of C, H-spin-coupling constants. Helv. Chim. Acta 1987, 61, 607–617.

33. Ashooriha, M.; Khoshneviszadeh, M.; Khoshneviszadeh, M.; Rafiei, A.; Kardan, M.; Yazdian-Robati, R.; Emami, S. Kojic acid-natural product conjugates as mushroom tyrosinase inhibitors. Eur. J. Med. Chem. 2020, 201, 112480.

34. Larik, F.A.; Saeed, A.; Channar, P.A.; Muqadar, U.; Abbas, Q.; Hassan, M.; Seo, S.Y.; Bolte, M. Design, synthesis, kinetic mechanism and molecular docking studies of novel 1-pentanoyl-3-arylthioureas as inhibitors of mushroom tyrosinase and free radical scavengers. Eur. J. Med. Chem. 2017, 141, 273–281.

35. Choi, I.; Park, Y.; Ryu, I.Y.; Jung, H.J.; Ullah, S.; Choi, H.; Park, C.; Kang, D.; Lee, S.; Chun, P.; et al. In silico and in vitro insights into tyrosinase inhibitors with a 2-thioxooxazoline-4-one template. Comput. Struct. Biotechnol. J. 2021, 19, 37–50.

36. Chung, K.W.; Jeong, H.O.; Jang, E.J.; Choi, Y.J.; Kim, D.H.; Kim, S.R.; Lee, K.J.; Lee, H.J.; Chun, P.; Byun, Y.; et al. Characterization of a small molecule inhibitor of melanogenesis that inhibits tyrosinase activity and scavenges nitric oxide (NO). Biochim. Biophys. Acta 2013, 1830, 4752–4761.

37. Lineweaver, H.; Burk, D. The determination of enzyme dissociation constants. J. Am. Chem. Soc. 1934, 56, 658–666.

38. Morris, G.M.; Huey, R.; Lindstrom, W.; Sanner, M.F.; Belew, R.K.; Goodsell, D.S.; Olson, A.J. AutoDock4 and AutoDockTools4: Automated docking with selective receptor flexibility. J. Comput. Chem. 2009, 30, 2785–2791.

39. Trott, O.; Olson, A.J. AutoDock Vina: Improving the speed and accuracy of docking with a new scoring function, efficient optimization, and multithreading. J. Comput. Chem. 2010, 31, 455–461.

40. Heitz, M.P.; Rupp, J.W. Determining mushroom tyrosinase inhibition by imidazolium ionic liquids: A spectroscopic and molecular docking study. Int. J. Biol. Macromol. 2018, 107, 1971–1981.

41. Battaini, G.; Monzani, E.; Casella, L.; Santagostini, L.; Pagliarin, R. Inhibition of the catecholase activity of biomimetic dinuclear copper complexes by kojic acid. J. Biol. Inorg. Chem. 2000, 5, 262–268.

42. Ujan, R.; Saeed, A.; Ashraf, S.; Channar, P.A.; Abbas, Q.; Rind, M.A.; Hassan, M.; Raza, H.; Seo, S.Y.; El-Seedi, H.R. Synthesis, computational studies and enzyme inhibitory kinetics of benzothiazole-linked thioureas as mushroom tyrosinase inhibitors. J. Biomol. Struct. Dyn. 2020, 1–9.

43. Xiong, S.L.; Lim, G.T.; Yin, S.J.; Lee, J.; Si, Y.X.; Yang, J.M.; Park, Y.D.; Qian, G.Y. The inhibitory effect of pyrogallol on tyrosinase activity and structure: Integration study of inhibition kinetics with molecular dynamics simulation. Int. J. Biol. Macromol. 2019, 121, 463–471.

44. Saeed, A.; Mahesar, P.A.; Channar, P.A.; Abbas, Q.; Larik, F.A.; Hassan, M.; Raza, H.; Seo, S.Y. Synthesis, molecular docking studies of coumarinyl-pyrazolinyl substituted thiazoles as non-competitive inhibitors of mushroom tyrosinase. Bioorg. Chem. 2017, 74, 187–196.
45. Raza, H.; Abbasi, M.A.; Siddiqui, S.Z.; Hassan, M.; Abbas, Q.; Hong, H.; Shah, S.A.A.; Shahid, M.; Seo, S.Y. Synthesis, molecular docking, dynamic simulations, kinetic mechanism, cytotoxicity evaluation of N-(substituted-phenyl)-4-{(4--1-piperazinyl} butanamides as tyrosinase and melanin inhibitors: In vitro, in vivo and in silico approaches. Bioorg. Chem. 2020, 94, 103445.
46. Pelle, E.; Mammone, T.; Maes, D.; Frenkel, K. Keratinocytes act as a source of reactive oxygen species by transferring hydrogen peroxide to melanocytes. J. Investig. Dermatol. 2005, 124, 793–797.
47. Hu, S.; Huang, J.; Pei, S.; Ouyang, Y.; Ding, Y.; Jiang, L.; Lu, J.; Kang, L.; Huang, L.; Xiang, H.; et al. Ganoderma lucidum polysaccharide inhibits UVB-induced melanogenesis by antagonizing cAMP/PKA and ROS/MAPK signaling pathways. J. Cell. Physiol. 2019, 234, 7330–7340.
48. Caldefie-Chézet, F.; Walrand, S.; Moinard, C.; Tridon, A.; Chassagne, J.; Vasson, M.P. Is the neutrophil reactive oxygen species production measured by luminol and lucigenin chemiluminescence intra or extracellular? Comparison with DCFH-DA flow cytometry and cytochrome c reduction. Clin. Chim. Acta 2002, 319, 9–17.
49. Becquet, F.; Courtois, Y.; Goureau, O. Nitric oxide decreases in vitro phagocytosis of photoreceptor outer segments by bovine retinal pigmented epithelial cells. J. Cell. Physiol. 1994, 159, 256–262.
50. Feelisch, M.; Ostrowski, J.; Noack, E. On the mechanism of NO release from sydnonimines. J. Cardiovasc. Pharmacol. 1989, 14, S13–S22.
51. Anouar, E. A Quantum chemical and statistical study of phenolic schiff bases with antioxidant activity against DPPH free radical. Antioxidants 2014, 3, 309–322.
52. Marc, G.; Atana, A.; Oniga, S.D.; Pirnau, A.; Vlase, L.; Oniga, O. New phenolic derivatives of thiazolidine-2,4-dione with antioxidant and antiradical properties: Synthesis, characterization, in vitro evaluation, and quantum studies. Molecules 2019, 24, 2060.
53. Corre, S.; Primot, A.; Sviderskaya, E.; Bennett, D.C.; Vaulont, S.; Goding, C.R.; Galibert, M.D. UV-induced expression of key component of the tanning process, the POMC and MC1R genes, is dependent on the p-38-activated upstream stimulating factor-1 (USF-1). J. Biol. Chem. 2004, 279, 51226–51233.
54. Oh, T.I.; Jung, H.J.; Lee, Y.M.; Lee, S.; Kim, G.H.; Kan, S.Y.; Kang, H.; Oh, T.; Ko, H.M.; Kwak, K.C.; et al. Zerumbone, a tropical ginger sesquiterpene of Zingiber officinale Roscoe, attenuates α-MSH-induced melanogenesis in B16F10 Cells. Int. J. Mol. Sci. 2018, 19, 3149.
55. Sun, L.; Guo, Y.; Zhang, Y.; Zhuang, Y. Antioxidant and anti-tyrosinase activities of phenolic extracts from rape bee pollen and inhibitory melanogenesis by cAMP/MITF/TYR pathway in B16 mouse melanoma cells. Front. Pharmacol. 2017, 8, 104.
56. Hirata, N.; Naruto, S.; Ohguchi, K.; Akao, Y.; Nozawa, Y.; Iinuma, M.; Matsuda, H. Mechanism of the melanogenesis stimulation activity of (−)-cubebin in murine B16 melanoma cells. Bioorg. Med. Chem. 2007, 15, 4897–4902.
57. Dong, Y.; Cao, J.; Wang, H.; Zhang, J.; Zhu, Z.; Bai, R.; Hao, H.; He, X.; Fan, R.; Dong, C. Nitric oxide enhances the sensitivity of alpaca melanocytes to respond to alpha-melanocyte-stimulating hormone by up-regulating melanocortin-1 receptor. Biochem. Biophys. Res. Commun. 2010, 396, 849–853.
58. Horikoshi, T.; Nakahara, M.; Kaminaga, H.; Sasaki, M.; Uchiwa, H.; Miyachi, Y. Involvement of nitric oxide in UVB-induced pigmentation in guinea pig skin. Pigment Cell Res. 2000, 13, 358–363.
59. Smalley, K.; Eisen, T. The involvement of p38 mitogen-activated protein kinase in the α-melanocyte stimulating hormone (α-MSH)-induced melanogenic and anti-proliferative effects in B16 murine melanoma cells. FEBS Lett. 2000, 476, 198–202.
60. Park, H.Y.; Kosmadaki, M.; Yaar, M.; Gilchrest, B.A. Cellular mechanisms regulating human melanogenesis. Cell. Mol. Life Sci. 2009, 66, 1493–1506.
61. Videira, I.F.; Moura, D.F.; Magina, S. Mechanisms regulating melanogenesis. An. Bras. Dermatol. 2013, 88, 76–83.
62. Hsu, K.D.; Chen, H.J.; Wang, C.S.; Lum, C.C.; Wu, S.P.; Lin, S.P.; Cheng, K.C. Extract of Ganoderma formosamum mycelium as a highly potent tyrosinase inhibitor. Sci. Rep. 2016, 6, 32584.